

Collapse of a Monolayer by Three Mechanisms

Christophe Ybert,[†] Weixing Lu, Gunter Möller, and Charles M. Knobler*

Department of Chemistry and Biochemistry, University of California, Los Angeles, California 90095-1569

Received: August 17, 2001; In Final Form: October 25, 2001

The collapse of monolayers of 2-hydroxytetracosanoic acid at the air/water interface has been examined by measurements of surface pressure–area isotherms and imaging with light scattering microscopy. Topographic images of films transferred to mica by the Langmuir–Blodgett technique have also been obtained. At low pressures, the films undergo “slow collapse” by the formation of multilayer islands. Folding occurs at high-pressure plateaus. At low compression rates, “giant folds” into the subphase arise at defects. They are composed of bilayers that remain suspended beneath the film and open reversibly during expansion. At higher rates of compression, the dominant collapse mechanism is by the formation of small-amplitude “multiple folds” that extend across the trough and are perpendicular to the compression direction.

The stability of insoluble monolayers at the air/water interface (Langmuir monolayers) is often discussed with reference to collapse, the process in which the 2D film undergoes a transition to a more stable 3D phase. This process can be thought of in the context of classical nucleation and growth. If the surface pressure of the film exceeds the equilibrium spreading pressure (π_{esp}), the pressure at which the monolayer is in equilibrium with the bulk phase, the monolayer becomes metastable. As the pressure is increased further, the barrier to nucleation decreases, and the formation of critical nuclei of the 3D phase becomes more probable. Once critical nuclei have formed, they grow into the bulk phase. Smith and Berg¹ showed that this picture could describe the decrease in the area of a monolayer with time when it was held at a constant pressure above π_{esp} . We will call this mechanism “slow collapse.” More recently, Vollhardt and collaborators² have used the same approach with specific models of the critical nucleus.

In many instances, however, monolayers collapse by the formation of trilayers (a bilayer on top of the monolayer) or multilayers rather than the bulk phase. This led Ries³ to propose that the collapse began with buckles in the film that grew to large amplitude, folded over, and then broke into disconnected multilayers. In what appears to be clear-cut evidence of this mechanism, electron micrographs of collapsed films of 2-hydroxytetracosanoic acid (2-OH TCA) showed a periodic array of lines that were characterized as ridges or folds perpendicular to the compression direction.⁴ Shadowing with platinum showed features 200 nm in height, which were interpreted as folds that had bent over toward the surface but remained attached to the underlying monolayer. Although collapse has often been attributed to the Ries mechanism, Nikomarov⁵ showed on energetic grounds that the mechanism was not viable in monolayers without defects. A stability analysis by Milner et al.⁶ demonstrated that a uniform monolayer film should become unstable with respect to buckling only at zero surface tension, i.e. only at a surface pressure $\pi \geq 72 \text{ mN m}^{-1}$. Measurements show that collapse occurs well before this limit. Inclusion of the spontaneous curvature in the expression for the free energy

of the film leads to a lower collapse pressure,⁷ but one that is still abnormally high. Recently, Diamant et al.⁸ proposed that buckling could arise at boundaries between monolayer phases as a result of instabilities that are related to height differences between phases of different spontaneous curvature.

Buckling has been observed in some recent experiments. Light-scattering⁹ and diffraction studies^{10,11} of very rigid monolayers have provided evidence for buckling instabilities with very small amplitude, on the order of 1–2 nm. Macroscopic, reversible buckling has been observed in a mixed monolayer containing the phospholipid DPPG and a protein and in pure DPPG monolayers on a subphase containing calcium ion.¹² The folding occurs in monolayers in which there is coexistence between an isotropic liquid phase and islands of a condensed phase. Large, isolated folds into the subphase begin at boundaries between the two phases. They remain connected to the monolayer and open reversibly when the film is expanded. More recently, Gopal and Lee¹³ have observed similar large-scale folding into the subphase in biphasic mixtures of DPPC and POPG. When the mixture becomes homogeneous above 33.5 °C, however, the collapse occurs by the formation of vesicles. Both folds and vesicles are observed between 28 and 33.5 °C.

Brewster-angle microscopy (BAM) images of the collapse of monolayers of behenic acid in a one-phase region show the presence of lines 30–50 μm wide.¹⁴ They have been taken to be ridges and not the formation of the three-dimensional phase. Schief et al.¹⁵ studied the collapse of DPPC by BAM and light-scattering microscopy (LSM) and observed the onset of static roughness at the boundaries between coalesced domains of the condensed phase. These “buds” form upward, away from the water and are 15–150 nm in height. They are reincorporated into the monolayer during expansion.

These experimental and theoretical results raise a number of questions. Can a global buckling instability be observed if a uniform monolayer is compressed to very high surface pressures? Does large-scale reversible buckling occur only in the presence of phase boundaries? How can the structure of folds observed in 2-OH TCA be squared with the theoretical analyses of stability? To address these questions we have re-examined the collapse in 2-OH TCA by measuring isotherms, following

* Corresponding author. E-mail: knobler@chem.ucla.edu.

[†] Current address: C.R.P.P., Av. Albert Schweitzer, 33600 Pessac, France.

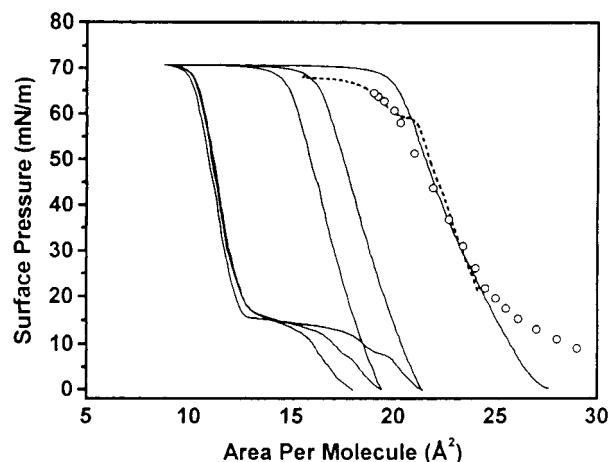


Figure 1. Surface pressure–molecular area isotherms of 2-OH TCA at 22 °C. The full lines show three successive compressions and expansions at $10 \text{ Å}^2 \text{ molecule}^{-1} \text{ min}^{-1}$, and the dashed line was measured at $0.6 \text{ Å}^2 \text{ molecule}^{-1} \text{ min}^{-1}$. The circles are taken from the data of Ries.⁴

the collapse by LSM and imaging films transferred to solid supports by atomic force microscopy (AFM).

Experimental Section

Samples of DL-2-OH TCA were obtained from Matreya and were claimed by the supplier to be 99+ % pure. Monolayers were spread from chloroform (Fisher, spectra-analyzed) solution onto Milli-Q water. Surface pressure–area isotherms were measured on a NIMA Type 611 trough equipped with a ribbon barrier. Pressure measurements were carried out with a filter-paper Wilhelmy plate.

The method for obtaining dark-field or light-scattering images is closely similar to that described by Schief et al.¹⁵ The monolayer, which was formed in a $5 \text{ cm} \times 20 \text{ cm}$ Teflon trough, was placed on the stage of a POLYVAR-MET microscope. It was illuminated by a 50 mW solid-state laser ($\lambda = 532 \text{ nm}$, Enlight Technologies, Model MGL-S) which struck the film obliquely. The direct beam was outside the field of view of the 20X objective, so only the scattered light was imaged. A silicon wafer in the subphase reflected the transmitted beam out of the field of view, and its polished surface minimized scattering. The images were captured by a CCD camera (Dage 772S) and recorded on videotape. Surface pressure was measured by a Wilhelmy plate with an R&K transducer and compression was carried out with a single Teflon barrier.

Langmuir–Blodgett monolayer films were prepared on freshly cleaved mica substrates by vertical dipping at a constant surface pressure. The dipping speed was 2 mm min^{-1} . Topographic images of the films were obtained with a scanning force microscope (Park Autoprobe) using 5 and 100 μm scanners. Microfabrication triangular silicon nitride cantilevers were employed. The images were obtained in the constant-force mode with loading forces in the range 1–3 nN.

Results

Isotherms. A typical pressure–area isotherm for 2-OH TCA on water at 22 °C and pH 4 is shown in Figure 1. The isotherm was recorded at a constant compression rate of $8 \text{ Å}^2 \text{ molecule}^{-1} \text{ min}^{-1}$. There is a sharp change in slope at 69 mN m^{-1} followed by a plateau. A sudden drop in the pressure occurs upon reexpansion followed by a plateau at about 20 mN m^{-1} . A loss of area is evident when the pressure reaches zero. Subsequent compression and expansion cycles follow the same pattern. The

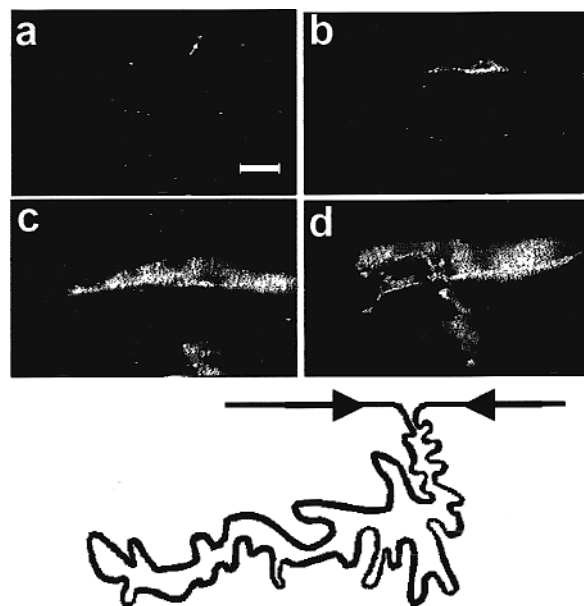


Figure 2. Formation of giant folds. This sequence of light-scattering microscope images was made at a compression rate of $0.8 \text{ Å}^2 \text{ molecule}^{-1} \text{ min}^{-1}$ and a pressure of 60 mN m^{-1} . Images b–d were obtained, respectively, at 3, 13, and 21 s after image a. The arrow in image a indicates the onset of the fold. Subduction of the monolayer occurs at the lower edge of the fold. A portion of another fold becomes visible in panel c; the folds are not connected. The bar represents 20 μm . A schematic of the fold cross section is also shown. The molecular tails, which would be in contact throughout the bilayer, are not shown.

isotherms change little when the compression rate is varied from about $1\text{--}25 \text{ Å}^2 \text{ molecule}^{-1} \text{ min}^{-1}$, but as shown by the dashed line, a plateau at 60 mN m^{-1} becomes evident, and the maximum pressure achieved before collapse is lower when the compression is slower. The significance of these changes will be discussed later. Also shown in the figure are points taken from the isotherm reported by Ries⁴ at 22 °C and pH 7; the compression rate was unspecified. There is generally good agreement at high pressures, but the collapse pressure is slightly lower, 68 mN m^{-1} . The Ries isotherm also falls off much more slowly at areas greater than $25 \text{ Å}^2 \text{ molecule}^{-1}$. We observe a similar shape in isotherms of solutions that have not been freshly prepared.

Imaging Studies. Dark-field images of a 2-OH TCA monolayer during slow compression are shown in Figure 2. A few bright spots are visible even at the lowest pressures despite efforts to keep the system dust free; their number grows as the pressure increases. AFM images (see below) show that these are regions of multilayer, which we believe are formed by slow collapse. At a compression rate of $0.8 \text{ Å}^2 \text{ molecule}^{-1} \text{ min}^{-1}$, isolated folds, which we call “giant folds” begin to appear at pressure of 60 mN m^{-1} . The folds are initially short segments but they grow in length and amplitude as the compression continues. When a fold is forming, fluctuations in its shape and size cause it to shimmer; they die out when the fold stops growing, leaving a static crumpled structure. The folds are generally not straight and display no preferred orientation. The LSM images are projections through the film. By focusing into the subphase, it is possible to bring successive parts of the fold into view, demonstrating that the folds project into the subphase rather than into the air. Subduction of the monolayer into the fold is evident from the motions of the bright spots formed by slow collapse. If the paths of individual spots are followed, it

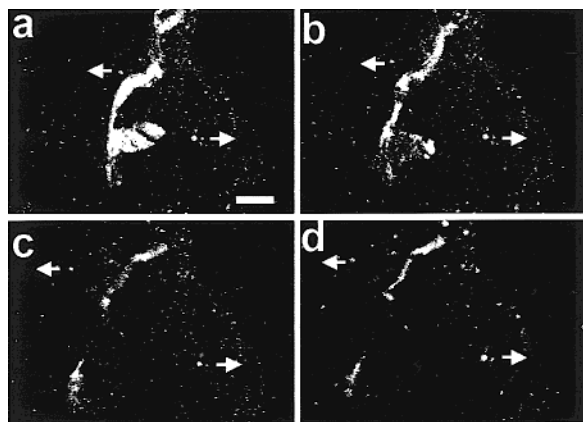


Figure 3. Expansion of a giant fold at a rate of $0.8 \text{ molecule}^{-1} \text{ min}^{-1}$. The time between successive images was 10 s. Only a portion of the expansion is shown; it leaves no trace when it is complete. Transfer of material from the fold to the monolayer can be followed from the motions of the multilayer islands, two of which are shown by arrows. The bar represents $20 \mu\text{m}$.

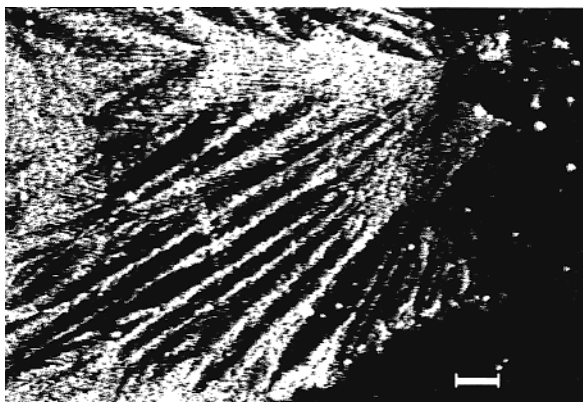


Figure 4. Portion of a giant fold in which folds are evident. Not all regions of the fold can be brought into focus at the same time. The bar represents $20 \mu\text{m}$.

is clear that the film is usually drawn into the subphase only along a narrow line at the surface, as shown in the sketch in Figure 2.

The folded regions extend deeply into the subphase, projecting as much as a few tens of micrometers and extending for several hundred micrometers. They are anchored at the monolayer and bend beneath it. If the subphase is disturbed, the giant folds can be seen to move with respect to the bright spots that define the position of the monolayer, and sometimes they detach from the monolayer and drift freely within the subphase.

Folds open during the expansion at the lower plateau, as shown in Figure 3. The process begins when an inactive fold begins to shimmer and is complete when the fold has vanished, leaving no obvious trace. When the film is recompressed, folds reappear close to the places in which they were formed during the first compression, suggesting that they are initiated at defects. During the unfolding process, folds move beneath the subphase as they are drawn up to their point of attachment to the monolayer. In some rare instances, folds appear to have a tubular structure much like a stocking whose boundary with the monolayer is circular rather than linear. Regions of closely spaced lines are often evident in the giant folds, as in Figure 4, showing that they consist of multiply folded portions. The amount of material in a fold can be estimated by tracing the motions of the slow-collapse dots. In the absence of a fold, we observe that the relative expansion of a visible region of the

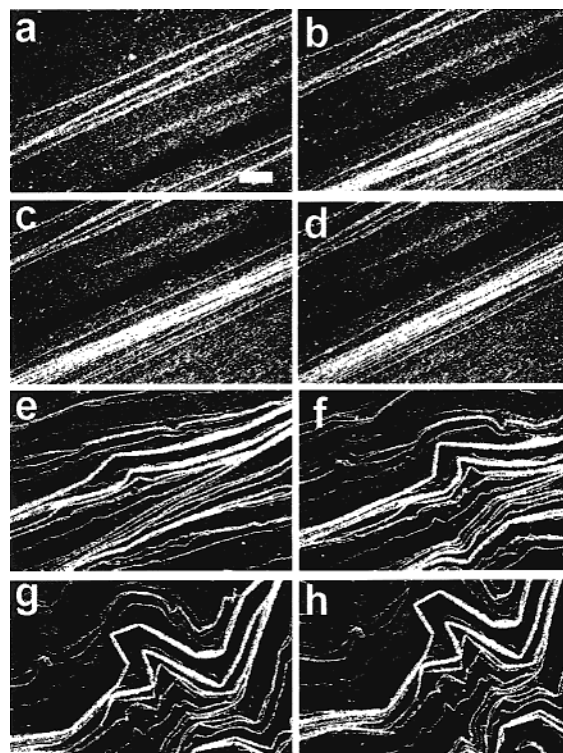


Figure 5. (a–d) The formation of multiple folds. This sequence of light-scattering microscope images was made at a compression rate of $1.6 \text{ Å}^2 \text{ molecule}^{-1} \text{ min}^{-1}$ and a pressure of 69 mN m^{-1} . Images b–d were obtained, respectively, at 7, 11, and 13 s after image a. The folds toward the top of the figures do not change significantly during the sequence, but there is a stepwise aggregation of thin folds toward the bottom that form a thick band. (e–h) Unfolding during expansion. Images f–h were obtained respectively at 14, 57 and 79 s after image e. The folds (not the same as those in a–d) were straight at the start of the expansion but became buckled as they separated. They eventually vanish.

monolayer is the same as the relative expansion of the entire film as determined by the movement of the barrier. On the other hand, the change in the local area around a respreading fold is larger because it includes the material that was stored in the fold. This excess area is 2.5–3.5 times the projected area of the fold before respreading, which is roughly consistent with a fold being made up of a highly crumpled bilayer.

Changes in the folding to structures that we call “multiple folds” become evident when the rate of compression is increased. As the pressure approaches 65 mN m^{-1} , scattering begins to be observed throughout the film. It becomes increasingly brighter and the film takes on a granular texture. As shown in Figure 5, which was obtained at a compression rate of $1.6 \text{ Å}^2 \text{ molecule}^{-1} \text{ min}^{-1}$, isolated long bright lines perpendicular to the compression direction appear suddenly ($<0.03 \text{ s}$) at 69 mN m^{-1} . More lines arise behind them, separated by about $10\text{--}20 \mu\text{m}$. Then, intermittently, lines suddenly move together. From the positions of the small bright spots within the film, it is apparent that these steps of about $20 \mu\text{m}$ are motions of rigid portions of the monolayer that either fold over or slide over each other. Typically, $10\text{--}30$ individual folds aggregate into a broad line. The folds do not remain active throughout the compression plateau; when the activity at one set of folds stops, folding can be found in another part of the film. The height of the multiple folds lies within the depth of field of the objective, so it is not possible to determine from the images whether the displacements of the monolayer are into or out of the subphase. If the compression is stopped, the pressure falls and the bright

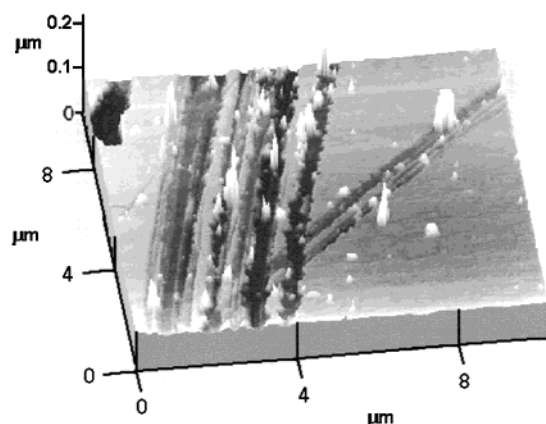


Figure 6. Topographic AFM image of a monolayer transferred to mica. In this image the multilayer islands range from 60 to 500 Å in height, but islands 2000 Å have been found in others. The ridges vary in depth from 35 to 75 Å, which is equivalent to 1–3 monolayers. The image has been smoothed but otherwise not treated.

background fades, but the folds remain. If the compression is restarted, the uniform background texture reappears.

The complex nature of the multiple folds is also evident upon expansion (Figure 5). In the lower-pressure plateau, broad bright lines separate continuously into from 10 to 30 parallel finer lines that move apart. As lines separate, they have the appearance of terraces. They do not remain straight but undergo a wavelike instability that grows in amplitude, and they evolve into irregular shapes that have the appearance of contour lines. With continued expansion, the lines fade and break up into small spots that disappear without obvious trace.

AFM Studies. A contact-mode AFM image of a collapsed monolayer of the ester acid on mica is shown in Figure 6. The LB transfer was performed in the plateau region. Visible is a section of a 4-μm-wide buckled region. The folds are not smooth, but there are large features that correspond roughly to multiples of the length of a fully extended molecule, 3 nm. The edges of the fold are clearly not a single monolayer high, which would be consistent with this region being part of a series of overlapping folds, several layers in thickness. In addition to the folds, there are multilayer islands 60–500 nm high. The width of the folds corresponds closely to those in Ries' electron micrograph images of 2-OH TCA.⁴ He assumed that all the very high features in the images were parts of ridges and that there were no multilayer islands. We think it more likely that the very high features in his images arose from the isolated islands.

Conclusions

Our experiments demonstrate that there are three distinct collapse mechanisms for 2-OH TCA, which depend on the surface pressure and the rate of compression. The formation of multilayer islands begins at low pressures but is very slow, which allows the other mechanisms to be studied. Smith and Berg¹ observed that the characteristic growth parameters for the collapse of fatty acids and alcohols depend on the chain length. At equivalent values of the supersaturation, $\pi - \pi_{\text{esp}}$, the growth rate for long-chain molecules is slower than that of their shorter chain homologues. For example, the growth rate parameter for eicosanol is 5 orders of magnitude smaller than that for octadecanol. Our success in observing folding is very likely attributable to the long chain length of 2-OH TCA.

If the rate of compression is sufficiently slow, giant folds appear that resemble those found in phospholipid mixtures^{8,12,13} in that they are reversible, directed into the subphase and 10–

100 μm in size. We know from both BAM images and X-ray grazing incidence diffraction studies¹⁶ that the folding occurs in a one-phase region of the phase diagram. This is in contrast to phospholipid monolayers, for which folding is observed when there is phase coexistence. Thus, a mechanism that depends on differences in height between phases of different spontaneous curvature⁸ can be ruled out. The folds are very likely stabilized by the strong van der Waals interactions between the molecular tails, and we believe that their size is eventually limited by the frictional forces that arise when the leaflets slide over each other. The dependence of the plateau pressure on the compression speed is related as well to this frictional cost of folding. More detailed isotherm studies of the methyl ester of 2-OH TCA^{17,18} and of 10,12-pentacosadiylic acid¹⁹ show this more clearly.

We have noted that the giant folds appear to be nucleated at monolayer defects. The X-ray diffraction studies¹⁶ show that the transition to an untilted phase occurs at 60 mN m⁻¹. Thus, the defects are not associated with molecular tilt; they may be dislocations.

In their initial stages, the multiple folds have some of the characteristics of the buckling instabilities that have been found in rigid films.^{9,10} They are always perpendicular to the compression direction and they extend across the trough. Multiple folds appear near the barrier rather than uniformly across the length of the film, which is probably the result of a surface pressure gradient. Although the multiple folds occur at high pressure, the surface tension remains too high to be consistent with the theoretical treatments of uniform films,^{6,7} and there is no evidence that they are associated with the defects that would be required for the Nikomarov mechanism⁵ for folding.²⁰ While we believe that the structures that we have observed by AFM correspond to the multiple folds observed in the floating monolayer, it is well-known that the morphology of a film can change when it undergoes an LB transfer. We cannot rule out that such changes have occurred, and one must be cautious as well about the electron micrographs obtained by Ries. However, the general characteristics of the AFM images are in accord with those obtained on the water surface by LSM, supporting the view that the transfer has occurred without a major loss in fidelity.

The formation of tubular, stocking-like folds has also been observed in a phospholipid mixture.¹³ Hu and Granek⁷ have found that a similar but periodic "long-finger" buckling can arise but they deem it "hardly relevant in the case of air-water interfaces" because it is unlikely to be stable against multilayer formation and it is found to occur at pressures in excess of the surface tension of water.

Like most of the other phenomena we have described, we have no understanding as yet of the origin of the quasi-two-dimensional buckling that accompanies the expansion of the multiple folds. It cannot be the instability in the domain boundaries predicted by Diamant et al.⁸ because it occurs in a one-phase system and there are no differences in spontaneous curvature that trigger the folding. Since the transition to an untilted phase occurs at 60 mN m⁻¹, we speculate that the instability in the multiple folds upon expansion is related to the appearance of molecular tilt at the lower expansion pressure.

Acknowledgment. This work was supported by the National Science Foundation. We thank S.B. Hall and K.Y.C. Lee for helpful discussions.

References and Notes

- (1) Smith, R. D.; Berg, J. C. *J. Colloid Inter. Sci.* **1980**, *74*, 273.

- (2) See, for example, Vollhardt, D. *Adv. Colloid Inter. Sci.* **1993**, 47, 1; Vollhardt, D.; Retter, U. *J. Phys. Chem.* **1991**, 95, 3723; Vollhardt, D.; Ziller, M.; Retter, U. *Langmuir* **1993**, 9, 3208.
- (3) Ries, H. E., Jr.; Kimball, W. A. *J. Phys. Chem.* **1955**, 59, 94.
- (4) Ries, H. E., Jr. *Nature* **1979**, 281, 287.
- (5) Nikomarov, E. S. *Langmuir* **1990**, 6, 410.
- (6) Milner, S. T.; Joanny, J.-F.; Pincus, P. *Europhys. Lett.* **1989**, 9, 495.
- (7) Hu, J.-G.; Granek, R. *J. Phys. II France* **1996**, 6, 999.
- (8) Diamant, H.; Witten, T. A.; Ege, C.; Gopal, A.; Lee, K. Y. C. *Phys. Rev. E* **2001**, 63, 061602. Diamant, H.; Witten, T. A.; Gopal, A.; Lee, K. Y. C. *Europhys. Lett.* **2000**, 52, 171.
- (9) Saint Jalmes, A.; Gallet, F. *Euro. Phys. J. B* **1998**, 2, 489; Saint-Jalmes, A.; Graner, F.; Gallet, F.; Houchmandzadeh, B. *Europhys. Lett.* **1994**, 28, 565.
- (10) Bourdieu, L.; Daillant, J.; Chatenay, D.; Braslau, A.; Colson, D. *Phys. Rev. Lett.* **1994**, 72, 1502.
- (11) Gourier, C. Thesis, University of Paris VI, Paris, France, 1996.
- (12) Lipp, M. M.; Lee, K. Y. C.; Takamoto, D. Y.; Zasadzinski, J. A. *Phys. Rev. Lett.* **1998**, 81, 1650.
- (13) Gopal, A.; Lee, K. Y. C. *J. Phys. Chem B* **2001**, 105, 10348.
- (14) Angelova, A.; Vollhardt, D.; Ionov, R. *J. Phys. Chem.* **1996**, 100, 10710.
- (15) Schief, W. R.; Touryan, L.; Hall, S. B.; Vogel, V. *J. Phys. Chem. B* **2000**, 104, 7388; Schief, W. R.; Hall, S. B.; Vogel, V. *Phys. Rev. E* **2000**, 62, 6831.
- (16) Brezesinski, G. **2001**. Private communication.
- (17) Sims, B.; Zografi, G. *J. Colloid Interface Sci.* **1972**, 41, 35.
- (18) Lu, W.; Ybert, C.; Möller, G.; Knobler, C. M. Manuscript in preparation.
- (19) Gourier, C.; Daillant, J.; Knobler, C. M.; Chatenay, M. D. Manuscript in preparation.
- (20) A referee has suggested that it may be possible to interpret the multiple folding as a phenomenon where the number of nuclei of the 3D phase are high and overlap to form larger structures. If this were so, one would be left with the question of how and why multilayer islands combine to form organized linear structures. Further, the AFM images show two distinct structures, very high multilayer islands, and much shallower folds.